

Advanced algorithms of extruded plastic fiber control for 3D printers

Evgeny A. Rybakov, Dmitry P. Starikov, Denis Y. Berchuk, Denis V. Zhuravlev

Institute of cybernetics
National Research Tomsk Polytechnic University, TPU
Tomsk, Russia
evgrybakov@gmail.com

Abstract — This paper describes methods and algorithms of setting plastic fiber extrusion unit. The scope of this article is automation of plastic fiber manufacture for 3D printing with implementation of advanced PID-algorithms, adaptive algorithms via the control vector redundancy.

Keywords – 3d printer; filament; PID-algorithm; fiber; extrusion.

I. INTRODUCTION

Nowadays, 3D printing gains the popularity and practical applicability. The most reasonable way of creating models is printing them out of ABS plastic. It is supplied in a printer in a form of filament (fig. 1).

The technology of plastic fiber production assumes the adherence of diameter (1.7 mm) with the accuracy of 30 mcm. The plants (extruders) that can provide the given value are expensive. The created model of an extruder is shown as a model in fig. 2.



Figure 1. Form of filament

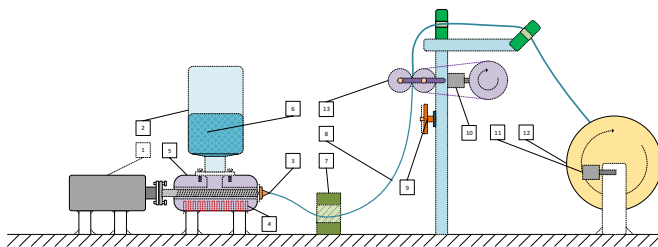


Figure 2. The model of extruder

where:

- | | |
|-----------------------|---------------------|
| 1 - Main motor; | 7 - Sensors; |
| 2 - Bunker; | 8 - Fiber; |
| 3 - A spinneret; | 9 - Cooler; |
| 4 - The heating coil; | 10 - Second motor; |
| 5 - Extruder; | 11 - Winding motor; |
| 6 - Atomized plastic; | 12 - Coil; |
| | 13 - Rollers. |

The crushed plastic is piled up to a special bunker (2) where it is heated up to the special temperature. The soft plastic is pressed out through the nozzle (3) as a filament (8) with a certain diameter by the screw rotating. After that, the fiber (8) extends through the position transducers (7) by the gravity method. Depending on the sensor reading (7), it is needed to control the motor rotating frequency (10). It is necessary to solve the following problems of controlling this SAC loop:

- The continuously adjustable frequency of a motor rotating (without working in fits and starts);
- The optimal speed search of broaching (due to the non-linear speed of plastic supplying from the extruder);
- The warning system support (the plastic break etc.).

Now the motor rotating frequency control is implemented with the help of relay automation. The use of such implementation involves only a partial solution to the tasks. For example, there is a probability of plastic break because of the motor impulse control. In addition, the diameter reduction is possible because of the fiber extension due to the stretching mechanism spurts.

II. MATHEMATICAL RATIONALE

During the device, operation identified the following factors affecting the exit diameter plastic:

- The number revolutions per minute of the main feed motor;
- The diameter of the plastic of the spinneret;
- The heating plastic temperature;
- The ambient temperature.

Obvious that the feeding effect angular velocity of the motor directly affect diameter of the plastic. Mathematically, this process can be described as:

$$(1) \quad d = k \cdot \omega_M.$$

The dependence has a simple linear form. Currently exploitation is conducted at a constant speed motor. But in implementing control via this parameter possible to detect some nonlinearities. The same effect of the inner diameter of the spinneret. This dependence is described by a similar manner. In general, the dependence of the diameter of the

hot plastic from the set of parameters described above is as follows:

$$d = k_1 \cdot \omega_M + k_2 \cdot d_f. \quad (2)$$

There are restrictions for the coefficients the equation. Changes in the internal diameter of the spinneret is performed manually (by simply replacing one nozzle to another). Therefore, this option is ignored for the description of the control action directly from of the spinneret, but it is essential in the formation of motor control algorithm. The next parameter - is heating temperature plastic. In a first approximation, determined that the temperature increase implies the decrease of the output diameter plastic ($\omega_{дБ} = \text{const}$).

$$d = \frac{k_3}{T_H} \quad (3)$$

Nowadays it is possible to reach the accuracy of 30 mcm on the functional plant but with the material over-expenditure, raising the question of profitability of the ABS fiber production.

III. ALGORITHMS

A. Adaptive PID-algorithm

The developed algorithm may solve the presented problems absolutely. It is based on the classical PID loop control and supposes the adaptive discrete control. The scheme of the classical PID loop control is shown in fig. 3.

The control influence is formed depending on the sensor (or sensors) feedback. It includes proportional, integral and differential components depending on the error value (the difference between a set point and a real value). The quality of processes depends on the respective factors selection (4).

$$u(t) = P + I + D = k_p e(t) + k_i \int_0^t e(\tau) d\tau + k_d \frac{de(t)}{dt} \quad (4)$$

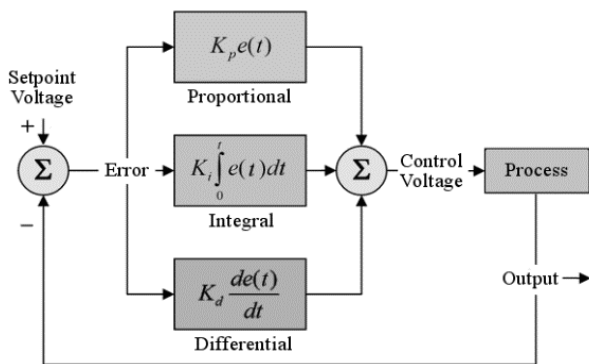


Figure 3. The classical scheme of the PID control loop

It is obvious that a classical PID controller assumes the continuous (analog) signal using. Moreover it does not support the control influence adaptation. The main task is the software and hardware complex for control speed of motor (pulling fiber) developing that allows avoiding jerks with the increasing speed, automatically selecting the optimal feeding speed.

When reading from the lowest sensor will reach the SETPOINT #1 the motor speed will increased according PID control algorithm. Before the highest SETPOINT #2 activation the algorithm of slowly breaking will be activated. Then the data for adaptive speed function will be saved and calculated. The calculated data will be transformed to the motor speed and translated to the engine. The motor will normally work at adaptive speed but if the highest sensor is activated at SETPOINT #3 the adaptive speed will be recalculated.

In general, the adaptive function may be presented as the following formula (5):

$$u_{i+1}(t) = \lim_{x \rightarrow t} \sum_{x=i-1}^{x=i} \frac{u_x}{2} \pm k_p e(t_{i-1}) + k_i \int_0^t e(\tau) d\tau + k_d \frac{de(t_{i-1})}{dt} \quad (5)$$

The choice of sum or difference shows depends on the motor speed trend. According to the algorithm the graphs of transients are presented in fig. 4. The research has given the following result (fig. 4).

According to the schedules of the transition process there is an ever-increasing and deceleration rotational speed of the broaching mechanism. Also, the algorithm provides the stable output for adaptive speed, which was calculated by a microcontroller using the trend process.

B. Advanced adaptive PID-algorithm

During operation of the device has been detected several factors, significantly complicating the task of selecting the optimal speed broaching mechanism (especially during start up). There are additional challenges:

- Automatic expansion / contraction limits for manipulated;
- Automatic quality analysis system transients and adjustment coefficients.

The algorithm provides a selection of optimum control action to assist starting the installation by changing the permissible limits of the mechanism. The condition of the lower and upper limits for motor control follows directly from the properties of the PWM controller. This limitation is contained in the function of counting rate adaptive.

The first algorithm is output to the adaptive rate previously described. The second, adds the flexibility and efficiency, has the following algorithmic structure:

A count frequency response of the upper / lower sensor for a certain period of time and stored in the variable.

Variable value obtained is compared with the empirical value, and if the number of positives is more, the new limit value is calculated by the formula:

$$\text{limit\#} = \text{limit\#} - k \times T, \quad (6)$$

where limit\# - count of the upper / lower limits;
 k - chosen transition coefficient;
 T - pulse repetition period of the sensor.

In accordance with the algorithm, charts of transients should look like (fig. 5).

C. The parametric reconfiguration

When the fiber first touches the upper or lower sensor (optocoupler), the coefficients of the controller remain the same (according to the initial values that were chosen experimentally, given the characteristics of the particular plastic (color, density)). After the first touch controller automatically decides to change the motor speed and the pulling time counting starts simultaneously to touch the next boundary (sensor). When the third time and subsequent times the fiber touches the sensor, then depending on the formulas (2), the coefficients of the controller are translated and thereby select the optimum engine speed, to fiber does not touch the sensor and did not commit a prolonged mechanism jerks.[1]

$$k_p^{i+1} = \frac{k_p^i}{t_i \cdot k}; \quad k_D^{i+1} = k_D^i \cdot k \cdot t_i; \quad k_I^{i+1} = \frac{k_I^i}{(t_0 - t_i \cdot k)}. \quad (7)$$

In accordance with the algorithm, charts of transients should look like (fig. 6).

D. The control vector redundancy

When the value from the lower of the sensor reached checkpoint, motor speed (broaching machine) begins to grow on the PID control algorithm, while motor speed slows extruder. Until the moment when the upper sensor is activated, the algorithm starts the slow deceleration of the working body. Thereafter special function saves and calculates parameters for the selection of an adaptive speed. Calculated data will be converted to the speed of rotation (extruder and broaching machine) and transferred motors. Drives will work on adaptive speed, but as soon as the upper sensor is activated again, the speed will be recalculated.

In accordance with the algorithm, charts of transients should look like (fig. 7).

Following the graphs, there is a smooth increase and decrease the speed of rotation broaching mechanism, as well algorithm provides access to adaptive speed calculated by the microcontroller based on trends.

IV. CONCLUSION

The described solutions have been tested and is successfully used in the ABS plastic fibers production in the upgraded unit. The solved problems:

- The smooth change of the engine speed (the pull mechanism) at the expense of transistor switches, PWM and the proposed algorithm.
- The optimal speed converting in the course of unit working is automatically selected.
- The emergencies were minimized because of the jolting pulling of fiber absence.

As the result of the comparison of the presented algorithms, there was made following statement: the fastest algorithm is appeared to be the parametric reconfiguration method. The control vector redundancy algorithm has showed the smoothest trends. But the best dynamic characteristics were obtained by the advanced adaptive PID-algorithm.

REFERENCES

- [1] Ziegler J.C. Nichols N.B. Optimum settings for automatic controllers. - USA: Research Triangle Park, 1992. - 759 p.
- [2] X. Luo, D. Liu, X. Guan, and S. Li, «Flocking in target pursuit for multi-agent systems with partial informed agents» IET Control Theory and Applications, vol. 6, no. 4, pp. 560–569, 2012
- [3] H. Su, X. Wang, and Z. Lin, «Flocking of multi-agents with a virtual leader» IEEE Transactions on Automatic Control, vol. 54, no. 2, pp. 293–307, 2009
- [4] Arduino Cookbook by Michael Margolis, Published by O'Reilly Media, Inc., 2011
- [5] Users Guide to Autodesk Inventor by Rajat K. Daftuar, Purdue University School of Electrical Engineering
- [6] Control System Design by Karl Johan Åström, 2002
- [7] R. Steele, Ed., «Fourth International Conference on Plastic Optical Fibers & Applications,” Information Gatekeeper, Boston, MA, USA, Oct. 17–19, 1995.
- [8] D. W. Van Krevelen, «Properties of Polymers,” 2nd ed, Elsevier, Amsterdam, 1976.
- [9] Bledzki A, Gassan J and Theis S. Wood-filled thermoplastic composites. Mech Compos Mater 1998; 34: 563–568.

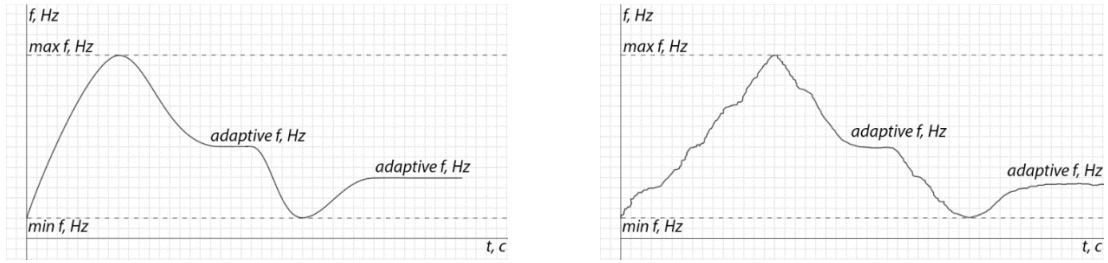


Figure 4. The graph of transient according to the algorithm and the real graph (from right) of transient.

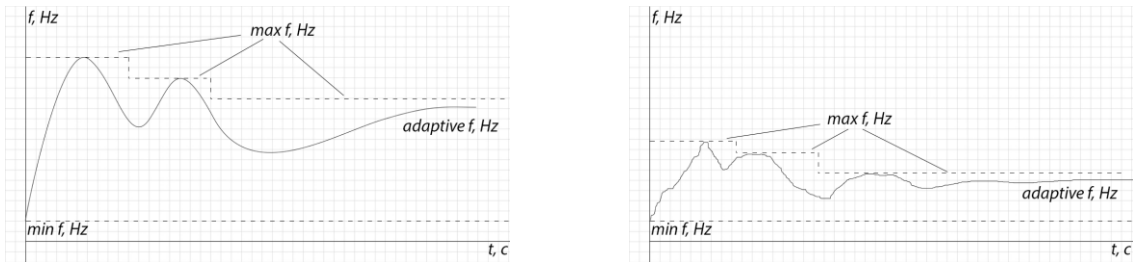


Figure 5. The graph of transient according to the algorithm and the real graph (from right) of transient.

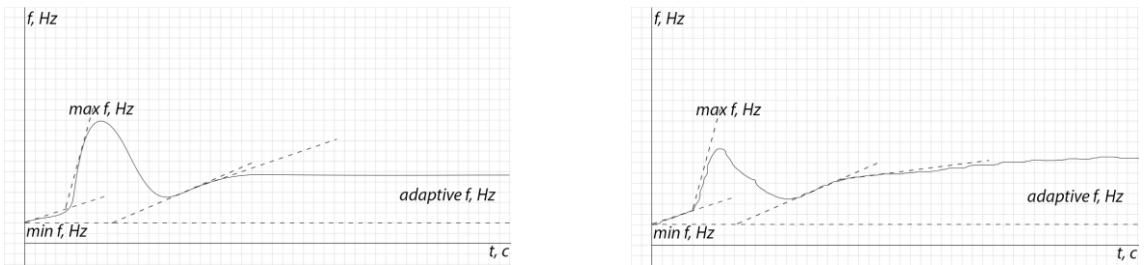


Figure 6. The graph of transient according to the algorithm and the real graph (from right) of transient.

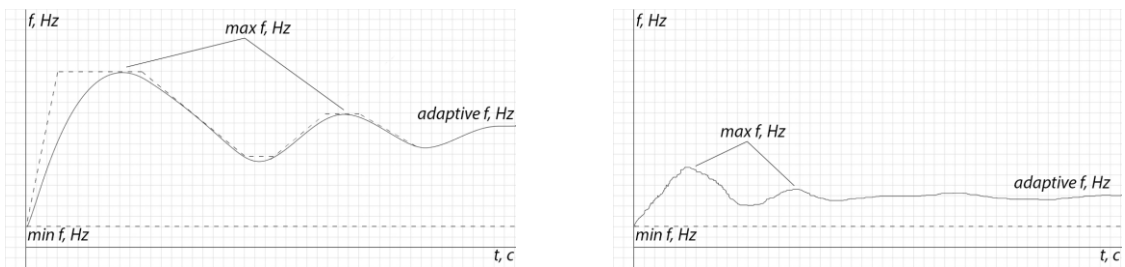


Figure 7. The graph of transient according to the algorithm and the real graph (from right) of transient.